

Theoretical Investigation of Group 4 Constrained-Geometry Complexes Featuring Phosphazene and Phosphinimido Arms

Lionel Truflandier,^[a] Colin J. Marsden,^[a] Christelle Freund,^[b] Blanca Martin-Vaca,^[b] and Didier Bourissou*^[b]

Keywords: Cations / Density functional calculations / Ligand Effects / Phosphorus / Zirconium

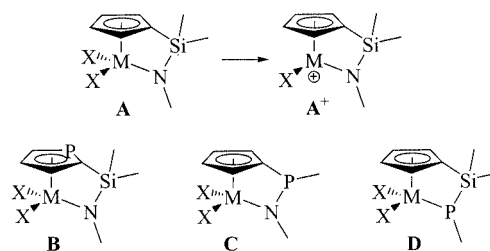
Density functional calculations are reported for the neutral and cationic forms of the “CpPN” zirconium complexes **E** and **F** featuring a phosphazene and phosphinimido pendant arm, respectively.

(© Wiley-VCH Verlag GmbH & Co. KGaA, 69451 Weinheim, Germany, 2004)

Introduction

The past 15 years have witnessed tremendous developments in the design and application of non-metallocene complexes as olefin polymerization catalysts.^[1] Spectacular achievements have been reported for the *ansa*-monocyclopentadienylsilylamido group IV catalysts, initially developed by Bercaw^[2a] and Okuda,^[2b] the so-called constrained-geometry catalysts (CGC) **A** (Scheme 1). Abstraction of one of the X ligands surrounding the metal centre provides the corresponding unsaturated d⁰ cationic complexes **A**⁺ that are generally agreed to be the catalytically active species in olefin polymerization.^[3] The applications of CGC catalysts are based not only on their electronic unsaturation, but also on their sterically unhindered reactive sites, combined with rigidity of the molecular framework and thermal stability. Of special interest is that the coordination of linear α -olefins is facilitated, allowing for their incorporation into polyethylene.

Numerous structural analogues of the initial “CpSiN” catalyst **A** have already been investigated by varying the nature of the cyclopentadienyl ligand,^[4] the bridging unit,^[5] the metal substituents^[6] and/or by replacing the amido group with another type of donor.^[7–9] Although phosphorus-containing complexes such as **B–D** have attracted considerable attention,^[10] the incorporation of a phosphazene or phosphinimido unit in constrained-geometry



Scheme 1. Structure of “CpSiN” complexes **A** and **A**⁺ and representative examples of related phosphorus-containing systems **B–D**

complexes has not yet been investigated. These phosphorus-containing nitrogen-based moieties are, however, common ligands for transition metals, whose properties can be readily be tuned by varying their substituents. Due to the highly polarized N^{δ−}–P^{δ+} bond, phosphazenes (R₃P=NR)^[11] are rather “hard” sp²-nitrogen donors that have recently been successfully involved in ethylene oligomerisation^[12a] as well as asymmetric cyclopropanation^[12b,12c] and allylic substitution.^[12d] Phosphinimido ligands (R₃P=N[−])^[13] possess a particularly versatile coordination chemistry. Their coordination to a single transition metal can involve from two to six electrons and result in linear as well as bent geometries. Their analogy with cyclopentadienyl ligands has been pointed out by Dehnicke^[14] and has been investigated by Stephan and co-workers for group IV complexes.^[15]

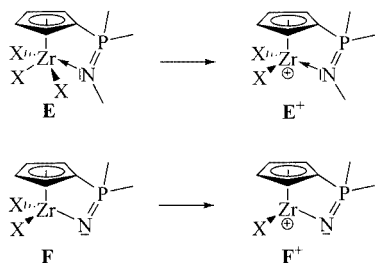
Here we report the theoretical investigation of two new “CpPN” models **E** and **F** (Scheme 2), featuring a pendant phosphazene and phosphinimido unit, respectively. DFT calculations were performed in order to determine if these constrained-geometry complexes deserve to be studied experimentally. For both models, the geometries of the neutral complexes as well as of their cationic analogues (derived by

^[a] Laboratoire de Physique Quantique du CNRS (UMR, 5626), IRSAMC, Université Paul Sabatier 118, route de Narbonne, 31062 Toulouse Cedex 04, France Fax: (internat.) +33-5/6155-6065

^[b] Laboratoire Hétérochimie Fondamentale et Appliquée du CNRS (UMR, 5069), Université Paul Sabatier 118, route de Narbonne, 31062 Toulouse Cedex 04, France Fax: (internat.) +33-5-6155-8204 E-mail: dbouriss@chimie.ups-tlse.fr

Supporting information for this article is available on the WWW under <http://www.eurjic.org> or from the author.

halide abstraction) were optimized. The resulting structural data and charges are discussed and compared with those of a model silicon-based complex of type **A**. During this study, particular emphasis has been placed upon the coordination of the phosphazene arm as well as substituent effects in complexes **E**.



Scheme 2. Structure of the phosphazene- and phosphinimido-based constrained geometry complexes **E** and **F**

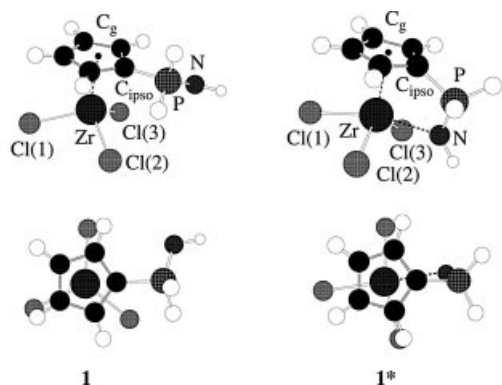
Results and Discussion

Complexes featuring a pendant phosphazene unit were first investigated both in the parent form and for various substitution patterns. Replacement of the phosphazene unit by a phosphinimido moiety was then studied for the parent form. For both model complexes, halide dissociation was evaluated geometrically and energetically.

Complexes Featuring a Pendant Phosphazene Unit $[\text{R}_2\text{P}(\eta^5\text{-C}_5\text{H}_4)(\text{R}'\text{N})\text{ZrX}_3]$ and $[\text{R}_2\text{P}(\eta^5\text{-C}_5\text{H}_4)(\text{R}'\text{N})\text{ZrX}_2]^+$

Parent Complex $[\text{H}_2\text{P}(\eta^5\text{-C}_5\text{H}_4)(\text{HN})\text{ZrCl}_3]$ (**1**)

Two energy minima were located on the potential energy hypersurface. The corresponding complexes **1** and **1*** are represented in Scheme 3, and selected geometric parameters are collected in Table 1.



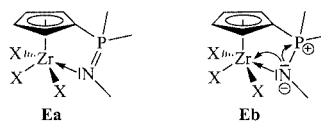
Scheme 3. Schematic representation (side and top views) of the B3LYP-optimized geometry of complexes **1** and **1***

In complex **1**, the phosphazene arm is in a position *cis* to the metal centre relative to the cyclopentadienyl ring (Cp)

(torsion angle $\text{Zr}-\text{C}_{\text{ipso}}-\text{P}-\text{N}$: 64.0° where C_{ipso} is the substituted carbon of the Cp ring, but not coordinated to the zirconium centre, as indicated by the $\text{Zr}-\text{N}$ distance (4.085 \AA). The environment around the zirconium centre is very similar to that of the model complex $[\text{CpZrCl}_3]$ (**2**), which is a more or less distorted tetrahedral geometry (“three-legged piano-stool”). As expected, the distance between the centroid (C_g) of the Cp ring and the metallic centre (2.265 \AA) is almost identical (2.242 \AA) to that observed for **2**.

The geometric parameters predicted for complex **1*** clearly indicate the rotation of the phosphazene arm (torsion angle $\text{Zr}-\text{C}_{\text{ipso}}-\text{P}-\text{N}$: 10.9°) and the presence of a $\text{Zr}-\text{N}$ interaction. Considering the centroid (C_g), the three chlorides and the nitrogen atom, the environment around the metal can be depicted by a pseudo-square-pyramidal (“four-legged piano-stool”^[16]) or trigonal bipyramidal structure. The constrained-geometry structure is indicated by the pyramidalization of C_{ipso} (sum of the bond angles $\Sigma = 352.9^\circ$ and $\text{C}_g-\text{C}_{\text{ipso}}-\text{P}$ angle = 158.1°). As a consequence, the C_g-Zr distance for **1*** (2.341 \AA) is significantly longer than that predicted for **1** (2.265 \AA). The $\text{Zr}-\text{Cl}$ distances are also elongated (**1***: 2.425 \AA on average; **1**: 2.373 \AA), but there is no preferential elongation of the $\text{Zr}-\text{Cl}$ bond in a position *trans* to the phosphazene unit in **1*** (2.432 \AA). The $\text{N}-\text{Zr}$ bond (2.357 \AA) is notably longer than that predicted for the unconstrained complex $[\text{CpZrCl}_3(\text{HN}=\text{PH}_3)]$ (**3**) (2.252 \AA) and the $\text{N}-\text{P}$ bond length in **1*** (1.613 \AA) is half-way between those of **1** (1.587 \AA) and **3** (1.633 \AA). All these data suggest only a weak coordination of the pendant arm.

The bonding interaction between the phosphazene and transition metal can be represented by two schematic forms **Ea** and **Eb** (Scheme 4). The phosphazene behaves only as a σ -donor in **Ea**, but both as a σ - and π -donor in **Eb**.^[17] The contribution of both σ - and π -type interactions in **1*** is clearly apparent from the appropriate orbitals localized according to the Boys method^[18] (Scheme 5).



Scheme 4. Schematic representations of complex **E**



Scheme 5. Isosurfaces for the localized molecular orbitals associated with σ and π $\text{N}-\text{Zr}$ overlaps

The coordination strength of the phosphazene arm may be estimated by the energy difference between **1** and **1***. The

phosphazene coordination was found to be favoured by ca. 8.4 kcal/mol^[19] (free enthalpy difference at 298 K, taking into account the vibrational and entropic corrections). This rather small value might result from the geometric constraint associated with the phosphazene coordination, or alternatively can be inherent to the coordination of the phosphazene to the CpZrCl₃ fragment. The latter hypothesis is supported by the only slightly larger value predicted for the coordination of the parent phosphazene HN=PH₃ to CpZrCl₃ leading to the unconstrained complex [CpZrCl₃(HN=PH₃)] (**3**; free enthalpy difference of 10.2 kcal/mol).

Substituent Effects: Complexes [R₂P(η⁵-C₅H₄)(R'N)-ZrX₃] (**4**–**7**)

Variation of the halide, phosphorus and nitrogen substituents was first investigated separately by geometry optimizations of complexes **4**-R, **5**-R' and **6**. For each complex, two energy minima were located on the potential energy hypersurface. The following discussion will be focussed on structures **4***–**6*** featuring a phosphazene-zirconium interaction (Table 2). The C_{ipso} pyramidalization and C_g–C_{ipso}–P bond angles are very similar in all complexes, suggesting that the geometric constraint is imposed by the framework and is essentially unaffected by the substituents. More significant modifications are observed for the Zr–N and N–P bond lengths. As far as the phosphorus substituents are concerned (complexes **4***-R), the Zr–N bond length decreases and the P–N bond length increases in the

series Cl/H/NH₂/CH₃/C₆H₅. The pronounced P–N bond shortening and Zr–N distance elongation on going from H to Cl can readily be related to the strong electron-withdrawing inductive effect (–I) of the chlorine atoms, which significantly decreases the electron density at the nitrogen^[20] and thus weakens the phosphazene-zirconium interaction. In contrast, the NH₂ (+M), CH₃ (+I) and C₆H₅ (+M) donor substituents (+M and +I for electron-donating mesomeric and inductive effects, respectively) increase the N^{δ–}P^{δ+} polarity of the P=N bond^[20] and thereby reinforce the phosphazene coordination. With regard to the nitrogen substituents, almost no structural modifications were observed with a methyl group, whereas introduction of an amino group induces a shortening of the Zr–N distance and an elongation of the P–N bond length. By analogy with that discussed for the phosphorus substituents, these modifications can be related to the +M effect of the amino group. Lastly, replacement of the chlorine by iodine atoms at zirconium (complex **6***) results in only negligible geometric modifications.

Substituent effects on the coordination strength of the phosphazene arm were then evaluated quantitatively. For all complexes **4**–**6**, except **4**-NH₂ (see below), the second minimum located on the energy surface is strongly related to **1**, with no interaction between the phosphazene and zirconium centre. As discussed previously, the coordination energy was thus obtained from the free enthalpy energy difference between the two energy minima (Table 3).

No energy minimum without interaction could be located for R = NH₂. Indeed, a stabilizing interaction between the

Table 1. Selected bond lengths (Å) and bond angles (°) for complexes **1**, **1*** and **2**

Complex	C _g –Zr ^[a]	Zr–Cl(1) ^[b]	Cl(2)–Zr–Cl(1) ^[b]
[H ₂ P(η ⁵ -C ₅ H ₄)(HN)ZrCl ₃] (1)	2.265	2.378	103.3
[H ₂ P(η ⁵ -C ₅ H ₄)(HN)ZrCl ₃] (1 *)	2.341	2.432	90.5
[(η ⁵ -C ₅ H ₄)ZrCl ₃] (2)	2.242	2.378	105.2

^[a] C_g denotes the centroid of the Cp ring. ^[b] See Scheme 3 for the notation (**1**, **2**).

Table 2. Selected bond lengths (Å) and bond angles (°) for complexes [R₂P(η⁵-C₅H₄)(R'N)ZrX₃] (**1***, **4***-R, **5***-R', **6*** and **7***)

Complex	Zr–N	N–P	Zr–X(1) ^[a]	Zr–X(2)	Zr–X(3)	C _g –Zr–N ^[b]	C _g –C _{ipso} –P ^[c]	C _{ipso} –P–N	Σ ^[d]	Zr–C _{ipso} –P–N
1 * (R = R' = H, X = Cl)	2.357	1.613	2.432	2.428	2.414	91.2	158.1	98.4	352.9	10.9
4 *-R (R' = H, X = Cl)										
Cl	2.456	1.578	2.411	2.405	2.405	90.9	159.4	100.7	353.9	0.6
NH ₂	2.319	1.616	2.441	2.438	2.475	91.2	159.2	95.9	353.0	18.1
CH ₃	2.307	1.625	2.443	2.448	2.426	91.7	158.6	96.7	352.9	9.6
C ₆ H ₅	2.298	1.626	2.447	2.429	2.453	91.1	158.3	96.5	353.0	1.6
5 *-R' (R = H, X = Cl)										
CH ₃	2.340	1.617	2.437	2.435	2.421	92.2	157.6	99.1	352.6	13.4
NH ₂	2.297	1.628	2.438	2.432	2.431	91.5	158.3	96.8	352.9	1.0
6 * (R = R' = H, X = I)	2.306	1.617	2.853	2.870	2.843	92.7	157.5	98.0	352.5	11.2
7 * (R = C ₆ H ₅ , R' = CH ₃ , X = I)	2.245	1.639	2.885	2.879	2.894	94.6	157.7	96.7	352.9	4.0

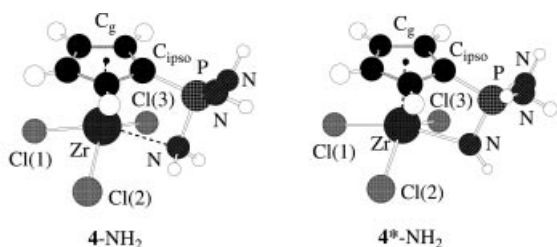
^[a] See Scheme 3 for the notation (**1**, **2**, **3**). ^[b] C_g denotes the centroid of the Cp ring. ^[c] C_{ipso} denotes the substituted carbon of the Cp ring. ^[d] Sum of bond angles around C_{ipso}.

Table 3. Estimated free enthalpy for the phosphazene-zirconium interaction ($\Delta_r G^\circ_{\text{N-Zr interaction}}$) in complexes $[\text{R}_2\text{P}(\eta^5\text{-C}_5\text{H}_4)(\text{R}'\text{N})\text{ZrX}_3]$ (**1***, **4*-R**, **5*-R'**, **6*** and **7***); negative values of $\Delta_r G^\circ_{\text{N-Zr interaction}}$ imply energetically favourable N–Zr interactions

Complex	Method 1 ^[a]	Method 2 ^[b]	Method 3 ^[b]
1* (R = R' = H, X = Cl)	–8.39	15.63	–8.49
4*-R (R' = H, X = Cl)			
Cl	–2.50	47.35	3.71
NH ₂	–8.05	8.98	–14.44
CH ₃	–14.68	6.54	–15.06
C ₆ H ₅	–16.94	11.77	–15.33
5*-R' (R = H, X = Cl)			
CH ₃	–10.38	16.00	–10.40
NH ₂	–15.78	9.56	–16.54
6* (R = R' = H, X = I)	–9.86	14.39	–9.73
7* (R = C ₆ H ₅ , R' = Me, X = I)	–19.48	9.40	–19.57

^[a] Method 1 refers to the energy difference between the two energy minima, with and without an N–Zr interaction. ^[b] Methods 2 and 3 refer to the isodesmic reactions 1 and 2, respectively.

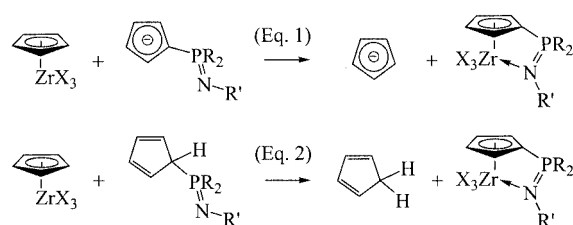
zirconium centre and one of the amino substituents at the phosphorus was observed for **4-NH₂** (Scheme 6). As a consequence, the coordination strength cannot be accurately estimated in this case by the energy difference between **4-NH₂** and **4*-NH₂**.



Scheme 6. Schematic representation of the B3LYP-optimized geometry of complexes **4-NH₂** and **4*-NH₂**

To circumvent this difficulty, we chose to evaluate the coordination energies through an isodesmic reaction.^[21,22] The coordination exchange between the anionic ligands $(\text{Cp})^-$ and $(\text{Cp-PR}_2=\text{NR}')^-$ was investigated first [Equation (1)]. The coordination was found to be endothermic $\{\Delta_r G^\circ_{\text{N-Zr interaction}}$ [Equation (1)] $> 0\}$ and the predicted values differ significantly from those obtained previously (Table 3). This divergence has tentatively been attributed to an electronic delocalization phenomenon, $\text{C}_{\text{ipso}} \rightarrow \text{P}$, within $(\text{Cp-PR}_2=\text{NR}')^-$. To confirm this hypothesis, coordination exchange between the corresponding neutral (protonated) ligands was then investigated [Equation (2)]. The resulting $\Delta_r G^\circ_{\text{N-Zr interaction}}$ [Equation (2)] values are now in very good agreement with those obtained previously (Method 1). Methods 1 and 3 differ significantly only in the case of **4*-Cl**, the value of $\Delta_r G^\circ_{\text{N-Zr interaction}}$ [Equation (2)] having probably been overestimated in this case due to the strong $-I$ effect of the chlorine atoms. For all other complexes, these two methods are almost perfectly correlated (slope: 0.97, correlation factor: 0.984), so that the coordi-

nation energy for R = NH₂ estimated using Equation (2) (14.4 kcal/mol) is likely to be reliable.



The value of $\Delta_r G^\circ_{\text{N-Zr interaction}}$ was found to be negative for all complexes **4*-6*** (from -16.9 to -2.5 kcal/mol). However, the phosphazene-zirconium interaction weakens significantly when chlorine atoms are introduced at phosphorus (**4*-Cl**: -2.5 kcal/mol compared to -8.4 kcal/mol for **1***), in agreement with previously discussed structural modifications. To a first approximation, the values of $\Delta_r G^\circ_{\text{N-Zr interaction}}$ are inversely proportional to the Zr–N bond lengths. Indeed, the substituents that induce the shorter Zr–N distances (NH₂, CH₃ and C₆H₅ at phosphorus, NH₂ at nitrogen) are associated with the larger coordination strengths (**4*-NH₂**: 14.4, **4*-CH₃**: 14.7, **4*-C₆H₅**: 16.9, **5*-NH₂**: 15.8 kcal/mol).

A more sophisticated complex was then studied in order to determine whether the various substituents have additive effects or not. A combination of iodine at zirconium, phenyl at phosphorus and methyl at nitrogen (complex **7***) results in the shortest N–Zr bond length (2.245 Å) and longest N–P bond length (1.639 Å) among all the complexes investigated (Table 2). The corresponding value of $\Delta_r G^\circ_{\text{N-Zr interaction}}$ (given by the energy difference between **7** and **7*** i.e. 19.5 kcal/mol) is more than twice as large as that for the parent complex (Table 3). This result suggests that the various substituents indeed have additive effects. This is further corroborated by the validity of Equation (3), in which the overall substituent effect in **7*** is expressed by the combination of related single-site terms (20.1 kcal/mol).

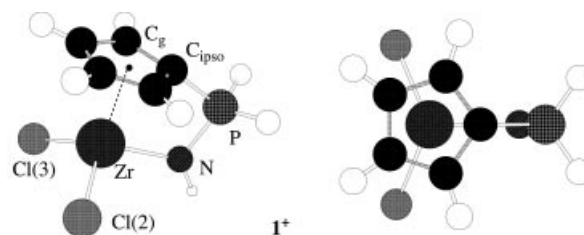
$$\Delta_r G^\circ_{\text{N-Zr interaction}}(\mathbf{7}^+) \approx \Delta_r G^\circ_{\text{N-Zr interaction}}(\mathbf{1}^+) + \Delta_r G^\circ_{\text{effect}}(\text{C}_6\text{H}_5) + \Delta_r G^\circ_{\text{effect}}(\text{CH}_3) + \Delta_r G^\circ_{\text{effect}}(\text{I}) \quad (\text{Eq. 3})$$

$$\begin{aligned} \text{with } \Delta_r G^\circ_{\text{effect}}(\text{C}_6\text{H}_5) &= \Delta_r G^\circ_{\text{N-Zr interaction}}(\mathbf{4}^+ - \text{C}_6\text{H}_5) - \Delta_r G^\circ_{\text{N-Zr interaction}}(\mathbf{1}^+), \\ \Delta_r G^\circ_{\text{effect}}(\text{CH}_3) &= \Delta_r G^\circ_{\text{N-Zr interaction}}(\mathbf{5}^+ - \text{CH}_3) - \Delta_r G^\circ_{\text{N-Zr interaction}}(\mathbf{1}^+), \\ \Delta_r G^\circ_{\text{effect}}(\text{I}) &= \Delta_r G^\circ_{\text{N-Zr interaction}}(\mathbf{6}^+) - \Delta_r G^\circ_{\text{N-Zr interaction}}(\mathbf{1}^+). \end{aligned}$$

Cationic Complexes $[\text{R}_2\text{P}(\eta^5\text{-C}_5\text{H}_4)(\text{R}'\text{N})\text{ZrX}_2]^+$ ($\mathbf{1}^+$ and $\mathbf{4}^+ - \mathbf{7}^+$)

Calculations were then performed on the cationic complexes obtained by dissociation of one of the halides. The coordination of the phosphazene arm is strongly favoured here by the high electrophilicity of the metallic centre. Accordingly, a single minimum was located on the energy hypersurface for the parent system $\mathbf{1}^+$ (Scheme 7, Table 4). The zirconium centre adopts a pseudo-tetrahedral geometry with C_s symmetry (planar environment around the nitrogen atom and eclipsed conformation of the phosphazene arm: $\text{Zr}-\text{C}_{\text{ipso}}-\text{P}-\text{N}$ dihedral angle of 0.2°). As expected, the halide dissociation induces a significant shortening of the $\text{Zr}-\text{N}$ bond ($\mathbf{1}^+$: 2.166 Å compared to $\mathbf{1}^*$: 2.357 Å) associated with a slight elongation of the $\text{N}-\text{P}$ bond ($\mathbf{1}^+$: 1.647 Å compared to $\mathbf{1}^*$: 1.613 Å). These modifications appear to have limited impact upon the coordination geometry, as suggested by the value of the $\text{C}_g-\text{C}_{\text{ipso}}-\text{P}$ bond angle ($\mathbf{1}^+$: 154.9° compared to $\mathbf{1}^*$: 158.1°).

The bridging $(\text{R}_2\text{P})^+$ and (R_2Si) fragments are isolobal, and the cationic phosphorus-bridged complex $\mathbf{1}^+$ was thus also compared to the neutral silicon-bridged complex $[\text{H}_2\text{Si}(\eta^5\text{-C}_5\text{H}_4)(\text{HN})\text{ZrCl}_2]$ ($\mathbf{8}$) (Table 5). Since the phosphorus and silicon atoms are almost identical in size, the geometric constraint is very similar ($\text{C}_g-\text{C}_{\text{ipso}}-\text{P}$ bond an-



Scheme 7. Schematic representation (side and top views) of the B3LYP-optimized geometry of complex $\mathbf{1}^+$

gle for $\mathbf{8}$: 154.5°). But, as expected, the $\text{Zr}-\text{N}$ bond is shorter in the neutral complex $\mathbf{8}$ (2.054 Å), which formally features a strongly donating silylamido arm.

According to NBO calculations (Table 6), the natural charges for the (NH) and (PH_2) fragments remain almost identical upon halide dissociation. In fact, the positive charge of $\mathbf{1}^+$ mainly develops on the metal centre (0.92 for the ZrCl_2 fragment in $\mathbf{1}^+$ compared to 0.16 for the ZrCl_3 fragment in $\mathbf{1}^*$). Interestingly, the charge distribution in $\mathbf{1}^+$ is half-way between those of the neutral and cationic silicon-bridged complexes $[\text{H}_2\text{Si}(\eta^5\text{-C}_5\text{H}_4)(\text{HN})\text{ZrCl}_2]$ ($\mathbf{8}$) and $[\text{H}_2\text{Si}(\eta^5\text{-C}_5\text{H}_4)(\text{HN})\text{ZrCl}]^+$ ($\mathbf{8}^+$) (0.74 for the ZrCl_2 fragment in $\mathbf{8}$ and 1.52 for the ZrCl fragment in $\mathbf{8}^+$). Complex $\mathbf{1}^+$, represented by schematic forms $\mathbf{E}^+ \mathbf{a}-\mathbf{c}$ (Scheme 8), can

Table 4. Selected bond lengths (Å) and bond angles ($^\circ$) for complexes $[\text{R}_2\text{P}(\eta^5\text{-C}_5\text{H}_4)(\text{R}'\text{N})\text{ZrX}_2]^+$ ($\mathbf{1}^+$, $\mathbf{4}^+ - \text{R}$, $\mathbf{5}^+ - \text{R}'$, $\mathbf{6}^+$ and $\mathbf{7}^+$)

Complex	Zr–N	N–P	Zr–X(2) ^[a]	Zr–X(3)	$\text{C}_g\text{–Zr–N}^{[b]}$	$\text{C}_g\text{–C}_{\text{ipso}}\text{–P}^{[c]}$	$\text{C}_{\text{ipso}}\text{–P–N}^{[d]}$	$\Sigma^{[d]}$	Zr–C _{ipso} –P–N
$\mathbf{1}^+$ (R = R' = H, X = Cl)	2.166	1.647	2.341	2.340	95.9	154.9	97.0	351.4	0.2
$\mathbf{4}^+ - \text{R}$ (R' = H, X = Cl)									
Cl	2.191	1.625	2.335	2.335	96.1	155.3	97.9	352.0	0.1
NH ₂	2.147	1.652	2.349	2.352	95.4	156.8	94.5	352.4	2.3
CH ₃	2.139	1.665	2.350	2.349	95.8	156.0	94.8	351.9	0.3
C ₆ H ₅	2.128	1.671	2.355	2.360	96.0	156.4	94.0	352.1	0.6
$\mathbf{5}^+ - \text{R}'$ (R = H, X = Cl)									
CH ₃	2.150	1.651	2.347	2.346	96.8	154.4	97.8	352.1	0.3
NH ₂	2.144	1.664	2.348	2.348	95.5	155.5	95.4	351.9	0.2
$\mathbf{6}^+$ (R = R' = H, X = I)	2.164	1.646	2.724	2.734	96.2	154.7	97.1	351.3	0.1
$\mathbf{7}^+$ (R = C ₆ H ₅ , R' = CH ₃ , X = I)	2.108	1.680	2.745	2.756	97.0	156.2	94.0	352.0	2.6

^[a] See Scheme 7 for the notation (2, 3). ^[b] C_g denotes the centroid of the Cp ring. ^[c] C_{ipso} denotes the substituted carbon atom of the Cp ring. ^[d] Sum of bond angles around C_{ipso} .

Table 5. Selected bond lengths (Å) and bond angles ($^\circ$) for complexes $[\text{H}_2\text{Si}(\eta^5\text{-C}_5\text{H}_4)(\text{HN})\text{ZrCl}_2]$ ($\mathbf{8}$) and $[\text{H}_2\text{Si}(\eta^5\text{-C}_5\text{H}_4)(\text{HN})\text{ZrCl}]^+$ ($\mathbf{8}^+$)

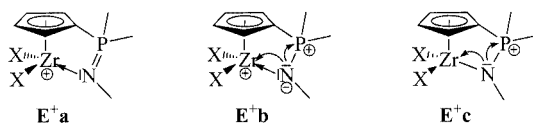
Complex	Zr–N	N–Si	Zr–Cl	$\text{C}_g\text{–Zr–N}^{[a]}$	$\text{C}_g\text{–C}_{\text{ipso}}\text{–Si}^{[b]}$	$\text{C}_{\text{ipso}}\text{–Si–N}$	$\Sigma^{[c]}$	Zr–C _{ipso} –Si–N
$[\text{H}_2\text{Si}(\eta^5\text{-C}_5\text{H}_4)(\text{HN})\text{ZrCl}_2]$ ($\mathbf{8}$)	2.054	1.756	2.399	98.6	154.5	92.5	350.2	0.0
$[\text{H}_2\text{Si}(\eta^5\text{-C}_5\text{H}_4)(\text{HN})\text{ZrCl}]^+$ ($\mathbf{8}^+$)	2.005	1.798	2.341	99.6	152.7	90.3	349.6	0.3

^[a] C_g denotes the centroid of the Cp ring. ^[b] C_{ipso} denotes the substituted carbon atom of the Cp ring. ^[c] Sum of bond angles around C_{ipso} .

Table 6. NBO charges^[7] for selected fragments of the parent complexes **1***, **1⁺**, **8**, **8⁺**, **9⁻**, **9** and **9⁺**

Complex	ZrCl _n	NH/N	PH ₂ /SiH ₂	Cp
[H ₂ P(η ⁵ -C ₅ H ₄)(HN)ZrCl ₃] (1*)	0.16	-0.90	1.39	-0.65
[H ₂ P(η ⁵ -C ₅ H ₄)(HN)ZrCl ₂] ⁺ (1⁺)	0.92	-0.88	1.49	-0.54
[H ₂ Si(η ⁵ -C ₅ H ₄)(HN)ZrCl ₂] (8)	0.74	-0.97	1.04	-0.81
[H ₂ Si(η ⁵ -C ₅ H ₄)(HN)ZrCl] ⁺ (8⁺)	1.52	-0.92	1.12	-0.72
[H ₂ P(η ⁵ -C ₅ H ₄)(N)ZrCl ₃] ⁻ (9⁻)	-0.18	-1.31	1.28	-0.78
[H ₂ P(η ⁵ -C ₅ H ₄)(N)ZrCl ₂] (9)	0.68	-1.30	1.35	-0.73
[H ₂ P(η ⁵ -C ₅ H ₄)(N)ZrCl] ⁺ (9⁺)	1.45	-1.25	1.44	-0.64

thus be considered as the cationic version of the “CpSiN” complex **A**.

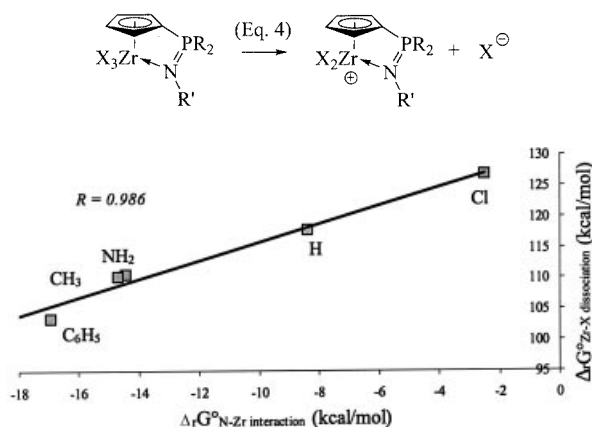
Scheme 8. Schematic representations of complex **E⁺**

The cationic complexes **4⁺–6⁺** featuring the various substitution patterns were then studied (Table 4). The resulting structural modifications are very similar to those observed for the neutral precursors **4*–6***. Comparison of the free enthalpies for the halide dissociation at 298 K in the gas phase [Equation (4)] yields a quantitative determination of the substituent effects (Table 7). As expected, the ionic dissociation of the neutral complexes **1*** and **4*–6*** is highly endothermic. The absolute values for $\Delta_r G^\circ_{\text{Zr-X dissociation}}$ cannot be discussed properly, since solvation and counteranion effects were not taken into account, although comparisons give more insight into the substituent effects. With regard to changes in the nature of the substituent at phosphorus (complexes **4⁺-R**), $\Delta_r G^\circ_{\text{Zr-X dissociation}}$ decreases along the series Cl > H > NH₂ > CH₃ > C₆H₅ with a maximum variation of 23.3 kcal/mol. The least and most favourable patterns for the halide dissociation are encountered by introduction of chlorine atoms and phenyl groups, respectively. These results parallel those observed for the phosphazene coordination (see above), and indeed, the in-

Table 7. Estimated free enthalpy change for the halide dissociation from neutral complexes [R₂P(η⁵-C₅H₄)(R'N)ZrX₃] (**1***, **4*-R**, **5*-R'**, **6*** and **7***) to the related cationic complexes [R₂P(η⁵-C₅H₄)(R'N)ZrX₂]⁺ (**1⁺**, **4⁺-R**, **5⁺-R'**, **6⁺** and **7⁺**)

Complex	$\Delta_r G^\circ_{\text{Zr-X dissociation}}$
1⁺ (R = R' = H, X = Cl)	117.9
4⁺-R (R' = H, X = Cl)	
Cl	126.7
NH ₂	110.7
CH ₃	110.2
C ₆ H ₅	103.4
5⁺-R' (R = H, X = Cl)	
CH ₃	115.7
NH ₂	119.7
6⁺ (R = R' = H, X = I)	95.3
7⁺ (R = C ₆ H ₅ , R' = CH ₃ , X = I)	80.5

fluence of the phosphorus substituents on the Zr–X dissociation is nicely correlated with that on the N–Zr interaction (Scheme 9). In marked contrast, introduction of an amino group at the nitrogen atom (**5*-NH₂**) induces a strong reinforcement of the Zr–N interaction, but only a small variation of $\Delta_r G^\circ_{\text{Zr-X dissociation}}$. In other words, the substituents at nitrogen have a much less pronounced effect on $\Delta_r G^\circ_{\text{Zr-X dissociation}}$ than those at phosphorus. Lastly, the halide dissociation is obviously more favourable for **6⁺** (X = iodine) than for **1⁺** (X = chlorine). Here again substituent effects are basically cumulative. Association of the most favourable substituents results in a decrease in $\Delta_r G^\circ_{\text{Zr-X dissociation}}$ by 37.4 kcal/mol for **7⁺** compared to **1⁺**.

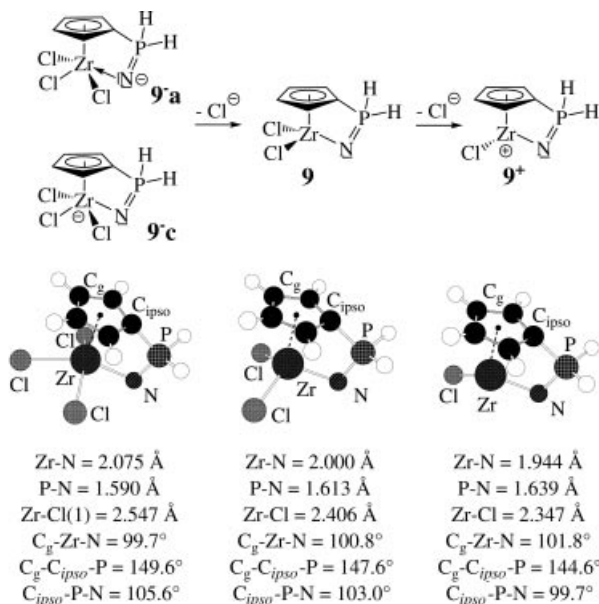
Scheme 9. Correlation of the influence of the phosphorus substituents on the N–Zr interaction and Zr–X dissociation; $\Delta_r G^\circ_{\text{N-Zr interaction}}$ determined with Method 1, except for R = NH₂ (Method 3)

Complexes Featuring a Pendant Phosphinimido Unit

[H₂P(η⁵-C₅H₄)(N)ZrCl₃]⁻ (**9⁻**), [H₂P(η⁵-C₅H₄)(N)ZrCl₂] (**9**) and [H₂P(η⁵-C₅H₄)(N)ZrCl]⁺ (**9⁺**)

Calculations were then carried out on the related complexes **9⁻**, **9** and **9⁺** featuring the dianionic ligand (Cp–PR₂=N)²⁻ and the ZrCl₃⁺, ZrCl₂²⁺ and ZrCl³⁺ fragments, respectively (Scheme 10). The presence of the strongly donating phosphinimido unit clearly favours the N–Zr interaction, which was observed for all these complexes.

Coordination of (Cp–PR₂=N)²⁻ to the ZrCl₃⁺ fragment does not induce the spontaneous dissociation of one chloride from the zirconium coordination sphere, and the anionic complex **9⁻** remains an energy minimum. The zirconium in **9⁻** adopts a pseudo-square-pyramidal environment, and the imido is inherently bent (Zr–N–P: 102.2°). The major difference concerns the N–Zr bond length, which is, as expected, considerably shorter in **9⁻** (2.075 Å) than in **1*** (2.357 Å). The reinforcement of this N–Zr interaction induces some increase in the geometry constraint, as illustrated by the bending of the C_g–C_{ipso}–P bond angle (**8⁻**: 149.6° compared to **1***: 158.1°). According to the NBO analysis, the excess negative charge is distributed over the ZrCl₃ fragment (–0.18) and the nitrogen atom (–1.31), in agreement with schematic structures **9⁻a** and **9⁻c** (Scheme 10).

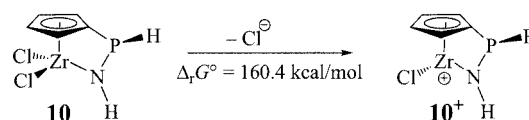


Scheme 10. Structure, schematic representation and selected geometric data of the B3LYP-optimized complexes **9^a**, **9** and **9⁺**

Not surprisingly, dissociation of one chlorine leads to the neutral complex **9**, featuring a pseudo-tetrahedral geometry. Chlorine dissociation is much more favourable for **9** ($\Delta_r G^\circ_{\text{Zr-X dissociation}} = 18.9$ kcal/mol) than for **1*** (117.9 kcal/mol). The N–Zr bond length (2.000 Å) is shorter than that of **9^a**, but the difference is significantly smaller than that predicted for the phosphazene-containing complexes **1**. Dissociation of a second chlorine affords the cationic complex **9⁺** featuring a pyramidal zirconium centre^[23] and a yet shorter N–Zr bond length (1.944 Å).

Complexes **9** and **9⁺** are strongly related to the silicon-bridged systems **8** and **8⁺**. The N–Zr bond lengths are only slightly shorter and the geometry constraint marginally higher in the phosphorus-bridged complexes. This analogy is corroborated by the similarity of both the NBO charges for the ZrCl₂ (**9**: 0.68/8: 0.74) and ZrCl (**9⁺**: 1.45/ **8⁺**: 1.52) fragments (Table 6) and the free enthalpies calculated for **9** → **9⁺** (155.2 kcal/mol) and **8** → **8⁺** (159.7 kcal/mol).

Lastly, phosphinimido-based complexes **F** were compared with their phosphinamido-based isomers **C**.^[10b] Isomerization between (NH)-aminophosphanes [R₂P(NH)R'] and (PH)-phosphazenes [R₂(PH)=NR'] is indeed a well-known process, including in metal complexes.^[24] Calculations were thus carried out on model complexes of type **C** and, accordingly, the phosphinamido complexes **10** and **10⁺** are predicted to be 25.7 and 20.6 kcal/mol more stable than the related phosphinimido complexes **9** and **9⁺** (Scheme 11). These values are in the same range as that reported by Schoeller for the free ligands (H₂P–NH)[–] and (H₃P=N)[–] (31 kcal/mol in favour of the NH tautomer).^[24d] The stabilization of the PH tautomer usually observed upon metal coordination is thus strongly balanced in this case by the ensuing increase in the geometric constraints (from **9** to **10** and **9⁺** to **10⁺**, the N–Zr and N–P bonds are noticeably elongated and the bending of C_{ipso} is significantly released).



Scheme 11. Structure and selected geometric data of the B3LYP-optimized complexes **10** and **10⁺**

Concluding Remarks

Theoretical investigations of phosphazene- and phosphinimido-based complexes **E** and **F** reveal numerous similarities but also noticeable differences with the “CpSiN” catalysts **A**. In particular, NBO natural charges suggest a significantly higher metal electrophilicity for **E** than for **A** (the positive charge is mainly localized on the ZrCl₂ fragment). Substituent effects are predicted to be additive and they influence strongly the structure and properties of both neutral and cationic complexes **E** and **E⁺**. Their influences on the N–Zr coordination strength and Zr–X dissociation appear to be strongly correlated, at least with respect to the nature of the phosphorus substituents. Phosphinimido-based complexes **F** are geometrically and electronically strongly related to the “CpSiN” catalysts **A**, but significantly more constrained than the related phosphinamido complexes **C**. Accordingly tautomerization of the parent complexes **9** → **10** and **9⁺** → **10⁺** is predicted to be energetically favoured.

These results as a whole suggest that constrained-geometry complexes featuring phosphazene and phosphinimido arms might indeed be interesting alternatives for the “CpSiN” catalysts. Accordingly, the interaction of complexes **E** and **F** with alkenes clearly deserves to be studied, and detailed investigations in this field are planned.

Computational Details

All calculations were carried out with the Gaussian 98^[25] suite of programs at the DFT level of theory using the hybrid functional B3LYP as implemented in that program.^[26,27] Halide, phosphorus, silicon and zirconium atoms were treated with the Averaged Relativistic Effective Core Potentials (AREPs) optimized by the Dresden-Stuttgart-Bonn group (Cl, I, P, Si^[28] and Zr^[29]). Basis sets adapted to the AREPs augmented with a d polarization function were used for the atoms of the p-block ($\exp_P = 0.387$, $\exp_{Si} = 0.284$,^[30] $\exp_{Cl} = 0.643$, $\exp_I = 0.730$ ^[31]) and an f polarization function was used for the zirconium atom ($\exp_{Zr} = 0.975$ ^[32]). Carbon, nitrogen and hydrogen were treated with an all-electron double- ζ 6-31G(d,p) basis set.^[33] Geometry optimiza-

tions were performed without spatial symmetry constraints and the nature of the extrema was verified by analytical calculations of vibrational frequencies. The atomic charges were obtained by NBO analyses.^[34]

Acknowledgments

Thanks are due to the CNRS, UPS and French Ministry of Research and New Technologies (ACI JC4091) for financial support of this work.

- [1] [1a] A. L. McKnight, R. M. Waymouth, *Chem. Rev.* **1998**, 98, 2587. [1b] G. J. P. Britovsek, V. C. Gibson, D. F. Wass, *Angew. Chem. Int. Ed.* **1999**, 38, 429. [1c] V. C. Gibson, S. K. Spitzmeyer, *Chem. Rev.* **2003**, 103, 283.
- [2] [2a] P. J. Shapiro, E. Bunel, W. P. Schaefer, J. E. Bercaw, *Organometallics* **1990**, 9, 867. [2b] J. Okuda, *Chem. Ber.* **1990**, 123, 1649.
- [3] For theoretical investigation of CGC mechanistic aspects, see: [3a] T. K. Woo, P. M. Margl, J. C. W. Lohrenz, P. E. Blöchl, T. Ziegler, *J. Am. Chem. Soc.* **1996**, 118, 13021. [3b] G. Lanza, I. L. Fragalà, T. J. Marks, *Organometallics* **2001**, 20, 4006. [3c] G. Lanza, I. L. Fragalà, T. J. Marks, *Organometallics* **2002**, 21, 5594.
- [4] [4a] S. Feng, J. Klosin, W. J. Kruper Jr, M. H. McAdon, D. R. Neithamer, P. N. Nickias, J. T. Patton, D. R. Wilson, K. A. Abboud, C. L. Stern, *Organometallics* **1999**, 18, 1159. [4b] A. J. Ashe, X. G. Fang, J. W. Kampf, *Organometallics* **1999**, 18, 1363. [4c] J. Klosin, W. J. Kluper Jr, P. N. Nickias, G. R. Roof, P. De Waele, K. A. Abboud, *Organometallics* **2001**, 20, 2663.
- [5] [5a] P. J. Sinnema, L. v. d. Veen, A. L. Spek, N. Veldman, J. H. Teuben, *Organometallics* **1997**, 16, 4245. [5b] P. T. Gomes, M. L. H. Green, A. M. Martins, *J. Organomet. Chem.* **1998**, 551, 133. [5c] L. Duda, G. Erker, R. Fröhlich, F. Zippel, *Eur. J. Inorg. Chem.* **1998**, 1153. [5d] D. van Leusen, D. J. Beestra, B. Hessen, J. H. Teuben, *Organometallics* **2000**, 19, 4084. [5e] H. Braunschweig, C. von Koblinski, U. Englert, *Chem. Commun.* **2000**, 1049. [5f] K. Kunz, G. Erker, S. Döring, R. Fröhlich, G. Kehr, *J. Am. Chem. Soc.* **2001**, 123, 6181. [5g] K. Kunz, G. Erker, S. Döring, S. Bredeau, G. Kehr, R. Fröhlich, *Organometallics* **2002**, 21, 1031. [5h] V. V. Kotov, E. V. Avtomonov, J. Sundermeyer, K. Harms, D. A. Lemenovskii, *Eur. J. Inorg. Chem.* **2002**, 678.
- [6] J. Jin, D. R. Wilson, E. Y. X. Chen, *Chem. Commun.* **2002**, 708.
- [7] [7a] F. Amor, A. Butt, D. E. du Plooy, T. P. Spaniol, J. Okuda, *Organometallics* **1998**, 17, 5836. [7b] J. Okuda, T. Eberle, T. P. Spaniol, V. Piquet-Faure, *J. Organomet. Chem.* **1999**, 591, 127. [7c] J. T. Park, S. C. Yoon, B. J. Bae, W. S. Seo, I. H. Suh, T. K. Han, J. R. Park, *Organometallics* **2000**, 19, 1269.
- [8] For simultaneous variation of the bridging unit and donor site, see: [8a] Y. X. Chen, P. F. Fu, C. L. Stern, T. J. Marks, *Organometallics* **1997**, 16, 5958. [8b] K. Kunz, G. Erker, G. Kehr, R. Fröhlich, H. Jacobsen, H. Berke, O. Blacque, *J. Am. Chem. Soc.* **2002**, 124, 3316. [8c] T. Ishiyama, T. Mizuta, K. Miyoshi, H. Nakazawa, *Organometallics* **2003**, 22, 1096. [8d] L. E. Turner, M. G. Thorn, P. E. Fanwick, I. P. Rothwell, *Chem. Commun.* **2003**, 1034.
- [9] For doubly bridged complexes, see: [9a] W. A. Herrmann, M. J. A. Morawietz, T. Priermeier, *Angew. Chem. Int. Ed. Engl.* **1994**, 33, 1946. [9b] J. Cano, P. Royo, M. Lanfranchi, M. A. Pellinghelli, A. Tiripicchio, *Angew. Chem. Int. Ed.* **2001**, 40, 2495. [9c] J. Cano, P. Royo, H. Jacobsen, O. Blacque, H. Berke, E. Herdtweck, *Eur. J. Inorg. Chem.* **2003**, 2463.
- [10] [10a] S. J. Brown, X. Gao, D. G. Harrison, L. Koch, R. E. v. H. Spence, G. P. A. Yap, *Organometallics* **1998**, 17, 5445. [10b] V. V. Kotov, E. V. Avtomonov, J. Sundermeyer, K. Harms, D. A. Lemenovskii, *Eur. J. Inorg. Chem.* **2002**, 678. [10c] G. Altenhoff, S. Bredeau, G. Erker, G. Kehr, O. Kataeva, R. Fröhlich, *Organometallics* **2002**, 21, 4084.
- [11] M. Witt, H. W. Roesky, *Chem. Rev.* **1994**, 94, 1163.
- [12] [12a] M. Sauthier, F. Leca, R. Fernando de Souza, K. Bernardo-Gusmão, L. F. T. Queiroz, L. Toupet, R. Réau, *New J. Chem.* **2002**, 26, 630. [12b] M. T. Reetz, E. Bohres, R. Goddard, *Chem. Commun.* **1998**, 935. [12c] J. M. Brunel, O. Legrand, S. Reymond, G. Buono, *J. Am. Chem. Soc.* **1999**, 121, 5807. [12d] M. Sauthier, J. Forniés-Cámer, L. Toupet, R. Réau, *Organometallics* **2000**, 19, 553.
- [13] [13a] K. Dehnicke, M. Krieger, W. Massa, *Coord. Chem. Rev.* **1999**, 182, 19. [13b] H. J. Cristau, M. Taillefer, N. Rahier, *J. Organomet. Chem.* **2002**, 646, 94.
- [14] [14a] T. Rubenstahl, F. Weller, S. Wacadlo, W. Massa, K. Dehnicke, *Z. Anorg. Allg. Chem.* **1995**, 621, 953. [14b] S. Anfang, K. Harms, F. Weller, O. Borgmeier, H. Lueken, H. Schilder, K. Dehnicke, *Z. Anorg. Allg. Chem.* **1998**, 624, 159.
- [15] [15a] D. W. Stephan, J. C. Stewart, F. Guérin, R. E. v. H. Spence, W. Xu, D. G. Harrison, *Organometallics* **1999**, 18, 1116. [15b] D. W. Stephan, F. Guérin, R. E. v. H. Spence, L. Koch, X. Gao, S. J. Brown, J. W. Swabey, Q. Wang, W. Xu, P. Zorick, D. G. Harrison, *Organometallics* **1999**, 18, 2046. [15c] J. E. Kickham, F. Guérin, J. C. Stewart, D. W. Stephan, *Angew. Chem. Int. Ed.* **2000**, 39, 3263. [15d] F. Guérin, C. L. Beddie, D. W. Stephan, R. E. v. H. Spence, R. Wurz, *Organometallics* **2001**, 20, 3466. [15e] N. Yue, E. Hollink, F. Guérin, D. W. Stephan, *Organometallics* **2001**, 20, 4424. [15f] C. Ong, J. Kickham, S. Clemens, F. Guérin, D. W. Stephan, *Organometallics* **2002**, 21, 1646. [15g] J. Kickham, F. Guérin, D. W. Stephan, *J. Am. Chem. Soc.* **2002**, 124, 11486. [15h] D. W. Stephan, J. C. Stewart, F. Guérin, S. Courtenay, J. Kickham, E. Hollink, C. Beddie, A. Hoskin, T. Graham, P. Wie, R. E. v. H. Spence, W. Xu, L. Koch, X. Gao, D. G. Harrison, *Organometallics* **2003**, 22, 1937. [15i] L. P. Spencer, R. Altwer, P. Wei, L. Gelmini, J. Gauld, D. W. Stephan, *Organometallics* **2003**, 22, 3841.
- [16] P. Kubáček, R. Hoffmann, Z. Havlas, *Organometallics* **1982**, 1, 180.
- [17] K. A. O. Starzewski, H. T. Dieck, *Inorg. Chem.* **1979**, 18, 3307.
- [18] S. F. Boys, *Rev. Mod. Phys.* **1960**, 32, 296.
- [19] At the suggestion of one of the referees, a few tests were performed with a larger basis set including diffuse functions either on nitrogen alone or both on nitrogen and carbon [6-31+G(d,p) instead of 6-31G(d,p)]. Changes of less than 0.01 Å were observed for the N–Zr bond lengths of complex **1*** and the coordination strengths decreased by only 1 kcal/mol.
- [20] W. C. Lu, C. C. Sun, *J. Mol. Struct. (Theochem)* **2002**, 593, 1.
- [21] P. George, C. W. Bock, M. Trachtman, *J. Chem. Ed.* **1988**, 61, 225.
- [22] W. J. Hehre, R. Ditchfield, L. Radom, J. A. Pople, *J. Am. Chem. Soc.* **1970**, 92, 4796.
- [23] L. Perrin, L. Maron, O. Eisenstein, *Faraday Discuss.* **2003**, 124, 25.
- [24] [24a] G. Schick, A. Loew, M. Nieger, K. Airola, E. Niecke, *Chem. Ber.* **1996**, 129, 211. [24b] G. Schick, M. Raab, D. Gudat, M. Nieger, E. Niecke, *Angew. Chem. Int. Ed.* **1998**, 37, 2390. [24c] S. Schulz, M. Raab, M. Nieger, E. Niecke, *Organometallics* **2000**, 19, 2616. [24d] M. Raab, A. Sundermann, G. Schick, A. Loew, M. Nieger, W. W. Schoeller, E. Niecke, *Organometallics* **2001**, 20, 1770. [24e] S. Schulz, T. Bauer, M. Nieger, I. Krossing, *Chem. Commun.* **2002**, 1422. [24f] T. Bauer, S. Schulz, M. Nieger, U. Kessler, *Organometallics* **2003**, 22, 3134.
- [25] M. J. Frisch, G. W. Trucks, H. B. Schlegel, G. E. Scuseria, M. A. Robb, J. R. Cheeseman, V. G. Zakrzewski, J. A. Montgomery, R. E. Stratmann, J. C. Burant, S. Dapprich, J. M. Millam, A. D. Daniels, K. N. Kudin, M. C. Strain, O. Farkas, J. Tomasi, V. Barone, M. Cossi, R. Cammi, B. Mennucci, C. Pomelli, C. Adamo, S. Clifford, J. Ochterski, G. A. Peterson, P. Y. Ayala, Q. Cui, K. Morokuma, D. K. Malick, A. D. Rabuck, K. Raghavachari, J. B. Foresman, J. Ciolowski, J. V. Ortiz, B. B. Stefanov, G. Liu, A. Liashenko, P. Piskorz, I. Nanayakkara, C.

- Gonzalez, M. Challacombe, P. M. W. Gill, B. G. Johnson, W. Chen, M. W. Wong, J. L. Andres, M. Head-Gordon, E. S. Replogle, et J. A. Pople. Gaussian 98, Revision A7, Gaussian Inc., Pittsburgh, PA, **1998**.
- [26] A. D. Becke, *J. Chem. Phys.* **1993**, 98, 5648.
- [27] C. Lee, W. Yang, R. G. Parr, *Phys. Rev.* **1988**, 37, B785.
- [28] A. Bergner, M. Dolg, W. Kuechle, H. Stoll, H. Preuss, *Mol. Phys.* **1993**, 80, 1431.
- [29] D. Andrae, U. Haeussermann, M. Dolg, H. Stoll, H. Preuss, *Theor. Chim. Acta* **1990**, 77, 123.
- [30] A. Höllwarth, M. Böhme, S. Dapprich, A. W. Ehlers, A. Gobbi, V. Jonas, K. F. Köhler, R. Stegmann, A. Veldkamp, G. Frenking, *Chem. Phys. Lett.* **1993**, 208, 237.
- [31] L. Maron, C. Teichteil, *Chem. Phys.* **1998**, 237, 105.
- [32] A. W. Ehlers, M. Böhme, S. Dapprich, A. Gobbi, A. Höllwarth, V. Jonas, K. F. Köhler, R. Stegmann, A. Veldkamp, G. Frenking, *Chem. Phys. Lett.* **1993**, 208, 111.
- [33] W. J. Hehre, R. Ditchfield, J. A. Pople, *J. Chem. Phys.* **1972**, 56, 2257.
- [34] [34a] NBO version 3.1. [34b] A. E. Reed, F. Weinhold, *J. Chem. Phys.* **1983**, 78, 1736. [34c] A. E. Reed, F. Weinhold, *J. Chem. Phys.* **1983**, 78, 4066. [34d] A. E. Reed, R. B. Weinstock, F. Weinhold, *J. Chem. Phys.* **1985**, 83, 735. [34e] A. E. Reed, L. A. Curtis, F. Weinhold, *Chem. Rev.* **1988**, 88, 899. [34f] E. D. Glendening, A. E. Reed, J. E. Carpenter, F. Weinhold, *J. Mol. Struct. (Theochem)* **1988**, 169, 41. [34g] J. P. Foster, F. Weinhold, *J. Am. Chem. Soc.* **1988**, 102, 7211.

Received October 21, 2003

Early View Article

Published Online March 30, 2004